Provided for non-commercial research and education use.
Not for reproduction, distribution or commercial use.

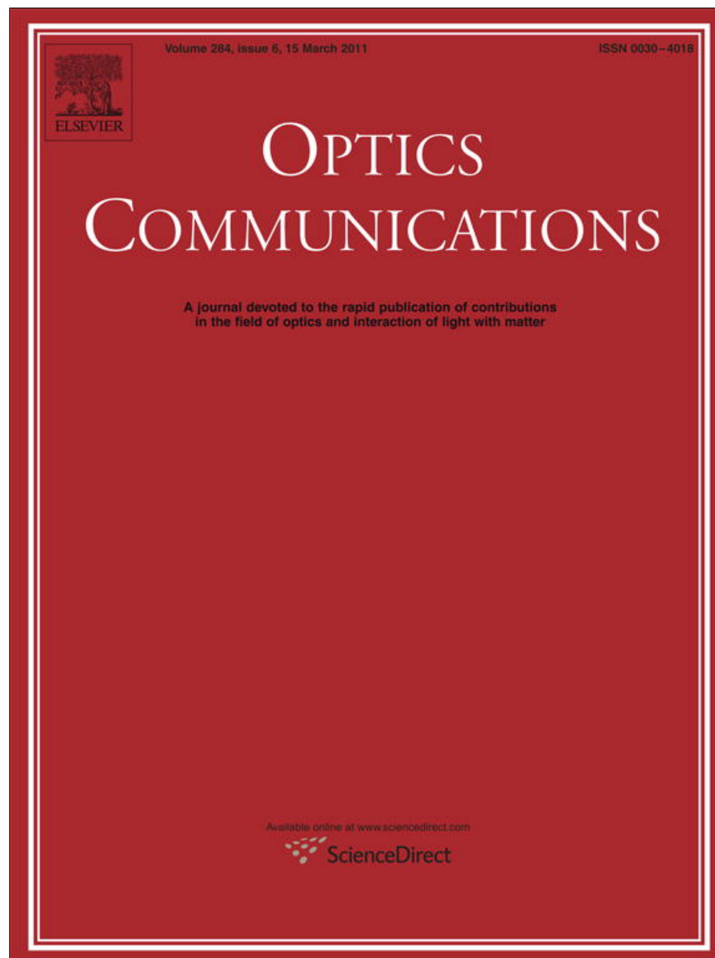

This article appeared in a journal published by Elsevier. The attached copy is furnished to the author for internal non-commercial research and education use, including for instruction at the authors institution and sharing with colleagues.

Other uses, including reproduction and distribution, or selling or licensing copies, or posting to personal, institutional or third party websites are prohibited.

In most cases authors are permitted to post their version of the article (e.g. in Word or Tex form) to their personal website or institutional repository. Authors requiring further information regarding Elsevier's archiving and manuscript policies are encouraged to visit:

http://www.elsevier.com/copyright

Author's personal copy

Optics Communications 284 (2011) 1677–1681

Contents lists available at ScienceDirect

Optics Communications

journal homepage: www.elsevier.com/locate/optcom

$AgGaS_2$- and Al-doped GaSe Crystals for IR Applications

Ying-Fei Zhang [a], Rong Wang [a], Zhi-Hui Kang [a], Li-Li Qu [a], Yun Jiang [a], Jin-Yue Gao [a], Yury M. Andreev [b], Grigory V. Lanskii [b,*], Konstantin A. Kokh [c], Alexander N. Morozov [b], Anna V. Shaiduko [b], Vladimir V. Zuev [b]

[a] Key Laboratory of Coherent Light and Atomic and Molecular Spectroscopy of Ministry of Education and College of Physics, Jilin University, Changchun, 130023, China
[b] Laboratory of Geosphere-Biosphere Interactions, Institute of Monitoring of Climatic and Ecological Systems SB RAS, Tomsk, 634055, Russia
[c] Laboratory of Crystal Growth, Institute of Geology and Mineralogy SB RAS, Novosibirsk, 630090, Russia

ARTICLE INFO

Article history:
Received 26 January 2010
Received in revised form 22 November 2010
Accepted 23 November 2010

Keywords:
Frequency conversion
SHG
Nonlinear crystal
GaSe
Doping

ABSTRACT

We report a systematic study of $AgGaS_2$- and Al-doped GaSe crystals in comparison with pure GaSe and S-doped GaSe crystals. $AgGaS_2$-doped GaSe (GaSe:$AgGaS_2$) crystal was grown by Bridgman technique from the melt of GaSe:$AgGaS_2$ (10.6 wt.%). Its real composition was identified as GaSe:S (2 wt.%). Al-doped GaSe (GaSe:Al) crystals were grown from the melt of GaSe and 0.01, 0.05, 0.1, 0.5, 1, 2 mass% of aluminium. Al content in the grown crystals is too small to be measured. The hardness of GaSe:S (2 wt.%) crystal grown from the melt of GaSe:$AgGaS_2$ is 25% higher than that of GaSe:S (2 wt.%) crystal grown by a conventional S-doping technique and 1.5- to 1.9-times higher than that of pure GaSe. GaSe:Al crystals are characterized by 2.5- to 3-times higher hardness than that of pure GaSe and by extremely low conductivity of $\leq 10^{-7}\,Om^{-1}\,cm^{-1}$. A comparative experiment on SHG in $AgGaS_2$-, Al-, S-doped GaSe and pure GaSe is carried out under the pumps of 2.12–2.9 μm fs OPA and 9.2−10.8 μm ns CO_2 laser. It was found that GaSe:S crystals possess the best physical properties for mid-IR applications among these doped GaSe crystals. GaSe:Al crystals have relatively low conductivity which have strong potential for THz application.

© 2010 Elsevier B.V. All rights reserved.

1. Introduction

ε-GaSe crystal, which is widely used in applied nonlinear optics, is a good matrix material for doping with various elements, such as S [1,2], In [3–5], Er [6–8], Al [9], and even $AgGaSe_2$ compound [4]. An original ε-polytype structure of GaSe is strengthened by doping and other physical properties responsible for the frequency conversion efficiency are also significantly modified. For example, In-doped GaSe (GaSe:In) crystals retain the transparency spectrum and phase matching (PM) angles with doping [3–5] but possess better nonlinear properties as compared with pure GaSe. Suhre et al. [3] showed that In-doping does not increase the intrinsic nonlinear properties in GaSe and the rise of nonlinearity occurred is due to the improvement of its optical quality. In case of GaSe doped with Er (0.5 atom%) the intrinsic nonlinearity is increased by 24% [6]. Simultaneously, the larger size of the erbium ions transforms the ends of the transparency spectrum, besides some broadening of the peak of an X-ray rocking curve. As a result, there are small differences between the measured data of PM angles in GaSe:Er and the estimated data with dispersion relations reported in [10] for pure GaSe.

Unlike other dopants, S-doping significantly shifts the transparency spectrum and the second harmonic generation (SHG) PM diagram to the short-wavelength range [2]. This shift of the short-wavelength cut in the transparency spectrum results in the decrease of the linear and the nonlinear absorption coefficient for the short-wavelength pumping. The decrease of PM angles increases the effective nonlinearity in negative GaSe of $\overline{6}2$ m point group symmetry. As a result, the SHG efficiency in GaSe:S (2 wt.%) crystals is much higher than that of pure GaSe crystals by modifying the optical, PM and thermal properties, and the damage threshold [2].

However, one of the most interesting attempts was to use the ternary $AgGaSe_2$ compound as a doping agent [4]. For GaSe doped with the 10.4 wt.% $AgGaSe_2$ compound, the nonlinear coefficient rises to the highest reported value of 75 pm/V among doped GaSe crystals. Hence, the effective nonlinear coefficient of this crystal is six times higher than that of $AgGaSe_2$ crystals and two times higher than that of $ZnGeP_2$ crystals [4]. Nevertheless, there are no details on the crystal composition, structure, physical properties, and PM for GaSe:$AgGaSe_2$ as well as for GaSe:Al crystals.

This article describes the optical properties and polytypic structure of the GaSe:Al (0.01, 0.05, 0.1, 0.5, 1, 2 wt.%) crystals grown by Bridgman technique and crystals grown from the melt of GaSe:$AgGaS_2$ (10.6 wt.%), which is the same in the conventional form: $Ag_{0.05}\,Ga_{0.95}Se_{1-x}S_x$, $x=0.1$ that we proposed as a prospective alternative to GaSe:$AgGaSe_2$. The SHG PM in $AgGaS_2$- and Al-doped crystals were studied at 2.12−2.9 μm and 9.2−10.8 μm under the pumping by a fs optical parametric amplifier (OPA) and ns CO_2 laser, respectively, at room temperature. Moreover, the same experimental conditions were also applied to the GaSe and GaSe:S (2, 10.2 wt.%) crystals for comparison.

* Corresponding author.
E-mail addresses: jygao@mail.jlu.edu.cn (J.-Y. Gao), lansky@yandex.ru (G.V. Lanskii).

0030-4018/$ – see front matter © 2010 Elsevier B.V. All rights reserved.
doi:10.1016/j.optcom.2010.11.067

Author's personal copy

For the nonlinear applications, GaSe:S crystals are attractive due to the optical properties and phase matching that could be controlled through S-content control on the stage of the crystal growth and that is why the appropriate properties of GaSe:S to GaSe:$AgGaS_2$ can be easily chosen for a comparative study. Unfortunately, the available experimental data on PM in GaSe:S crystals are limited and mainly focus on the SHG PM at Er^{3+}:YSGG (2.79 μm) and CO_2 laser (9.2−10.8 μm) pumping [1,2,11–16]. The SHG at 4.65 μm with fs OPG pumping is only mentioned in [15,16]. The difference frequency generation (DFG) of signal and idler waves by BBO optical parametric oscillator (OPO) at 5−19 μm range was realized in these crystals grown from the known charge composition but not the real composition [11]. Thus, these did not allow anyone to formulate an adequate full range dispersion equation. Therefore, this study could also provide some useful information for the design of full range dispersion equations for S-doped GaSe crystals.

2. Crystal growth and characterization

Pure and doped GaSe crystals were grown by the conventional Bridgman technique in evacuated quartz ampoules with the diameter of 18 mm. 6 N Ga and 6 N Se were the source components for GaSe crystals. 3 N Al, 3 N S and $AgGaS_2$ were doped inside the stoichiometric melt of GaSe. The temperature gradient on the crystallization front was 10 deg/cm and the crystal pulling rate was 6 mm/day. The charge compositions for crystal growth were as follows: GaSe:$AgGaS_2$ with 10.6 wt.% of $AgGaS_2$ or nominal composition—$Ag_{0.05}Ga_{0.95}Se_{0.9}S_{0.1}$ that is close to $Ag_{0.0463}Ga_{0.9573}Se_1$ crystal [4], GaSe:Al with 0.01, 0.05, 0.1, 0.5, 1, 2 wt.% of aluminum, and GaSe:S with 2, 10.2 wt.% of sulfur.

There was an intense segregation of Ag into the tail part of the GaSe:$AgGaS_2$ (10.6 wt.%) ingot that was about 2/3 of the whole ingot length. However, the nose part of the ingot is a high quality single crystal of a bright-red colour, which is similar to GaSe:S (2 wt.%) crystals described in [2]. The samples used in this study with the thickness of 20−25 μm, 65−75 μm, and 1±0.05 mm were cleaved from the grown ingots parallel to the c-plane layer and used without any additional treatment and polishing. The thickness of the GaSe:$AgGaS_2$ (10.6 wt.%) and GaSe:Al samples used in this study is ~0.3 mm. Many Al-rich scattering centres due to the intensive precipitation in GaSe:Al crystals were observed with Al concentrations greater than 0.05 wt.%. Doping composition and structure of the samples were studied by the electron probe micro-analysis and X-ray electron diffraction, respectively. Additionally, the bulk crystal structure was also identified by nonlinear technique. The crystal hardness was measured by the Nano Hardness Tester (CSEM, Switzerland).

The transparency spectra of the samples were measured over 32 times averaging by the spectrophotometer TU-1901 (Puing Corp., China) with spectral resolution $\Delta\lambda = 0.05$ nm in 0.2−0.9 μm range and ATAVAR 360 FT-IR spectrophotometer (ThermoNicolet) with $\Delta\nu = 4\ cm^{-1}$ in 2.5−25 μm range. The typical spectra of doped GaSe crystals are shown in Fig. 1. Transparencies of the samples were also carried out by point measurements with a low power ∅1.4 mm beam from the fs OPA at 2.6 μm, which could diminish the influence of the surface local defects on estimation of the absorption coefficient.

3. SHG experimental set-up

A conventional SHG optical set-up was used (Fig. 2). Pulse duration of homemade low-pressure line-tuneable CO_2 laser with TEM_{00} mode, 400−1000 Hz pulse-repetition rate and up to 500 W peak power was 150 ns in FWHM (full-width of half maximum) followed by 1 μs tail.

The sample (GaSe) was mounted on a step-motor-drive computer controlled rotational stage (RSA100, Zolix Instruments Co., Ltd, China). The rotational stage with positioning accuracy 18″ was located 1 m from the CO_2 laser. The CO_2 laser beam (∅3.5 mm) was focused by one BaF_2 lens (L_1, 65 mm focal length) on the crystal. The SHG beam was focused by the other BaF_2 lens (L_2, 65 mm focal length) on the pyroelectric

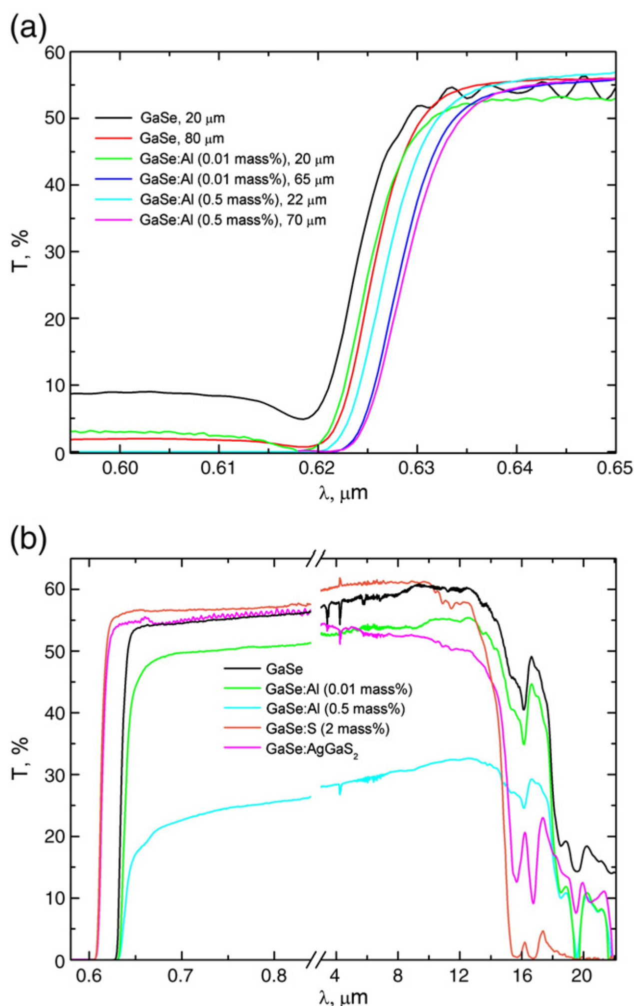

Fig. 1. (a) Short-wavelength transparency spectra for μm-thick films and (b) full range transparency spectra for 1-mm thick GaSe:Al, GaSe:S and GaSe samples and 0.35 mm GaSe:$AgGaS_2$, identified in the figure insets.

detector (R, MG-30, Russia, $D \geq 7 \times 10^8\ cm \cdot Hz^{1/2}/W$ at 2−20 μm range) which was used for SHG signal record. The residual CO_2 laser radiation was blocked by two LiF plates (F_1, F_2, 4 mm thickness) disposed close to the crystal (GaSe) and detector (R). The UV-FIR monochromator (Zolix SPB300, Beijing, China) with a diffraction grating of 66 gr/mm was used to monitor the CO_2 laser wavelength. SHG signals were recorded and averaged over 1000 pulses by the oscilloscope (Tektronix, TDS 2022).

The BBO OPA (Topas-C, Lithuana) was used as a second pump source. It generates 60−90 fs signal and idler pulses tuneable within 1.1−1.6 μm and 1.6−2.9 μm, respectively. The total average output power of the OPA

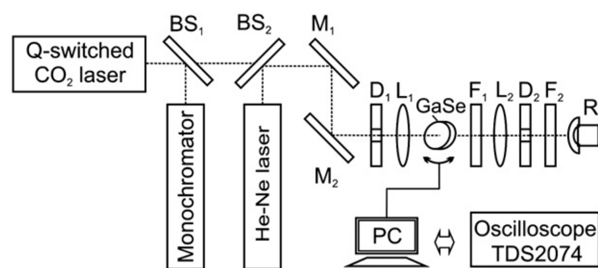

Fig. 2. Typical schematic SHG experimental setup with CO_2 laser pump. BS_1, BS_2, beam splitters; M_1, M_2, mirrors; F_1, F_2, LiF filters; D_1, D_2, diaphragms; L_1, L_2, BaF_2 lenses; R, MG-30 pyroelectric detector.

Author's personal copy

Topas-C output beam (∅1.4 mm) was ~0.5 W at ≤1% instability. PbS photoresistor (DPbS2900, Zolix, China) with $D \geq 5\times10^8$ cm·Hz$^{1/2}$/W, $\tau \leq 200$ μs, and voltage response ≥ 3×10^4 V/W at 0.8−2.9 μm range was used to detect the SHG signal.

4. Result and discussions

4.1. Chemical composition and physical properties

No noticeable quantity of Ag was found in the GaSe:$AgGaS_2$ sample but ~2 wt.% S is distributed more uniformly in contrast to the GaSe:S (2 wt.%) crystal grown by the conventional technique. The GaSe:S crystals (GaSe:$AgGaS_2$) have only 1−2% deficiency in S-content in reference to the charge composition. The low Al content and the overlapping of Al and Se X-ray reflexes prevent the measurement of Al content in GaSe:Al. Nevertheless, it was found that optical properties of GaSe degrade drastically at Al-doping level higher than 0.05 wt.% due to rich precipitation. Such samples are apparently useless for nonlinear applications.

It was found that GaSe:Al crystals possess the lowest conductivity of ≤10^{-7} Om^{-1} cm^{-1} along the (001) surface among all of the doped GaSe crystals and this is significantly attractive for the THz applications. It can be attributed to the substitution of Ga vacancies (which are p-type conductivity [17]) by Al leading to a rapid decrease in conductivity at low ≤0.01 wt.% doping. At higher Al-doping, however, Al may intercalate between layers to generate more minority carriers that keeps decreasing in the p-type conductivity.

GaSe:Al crystals possess the highest hardness among the doped GaSe crystals and the hardness linearly increases by increasing the Al-doping, namely 17 kg/mm^2 for 0.5 wt.% Al-doping and 22−24 kg/mm^2 for 2 wt.% Al-doping which is 2.5 to 3-fold higher than that of pure GaSe crystals and 1.25-fold to that of GaSe:S (2 wt.%) crystals grown by the conventional technique. It indicates that the smaller sized Al ions strengthen the lattice structure by occupying Ga vacancies, substituting larger sized Ga ions and/or by interstitial hardening. On the other hand, the higher hardness of GaSe:Al could be also partially caused by the Al intercalation between the growth layers leading to the formation of strong Al−Al bonds. For GaSe:$AgGaS_2$ crystals, the hardness is about 20 kg/mm^2 which is ~25% higher than that of GaSe:S (2 wt.%) crystals grown by the conventional technique and 1.5 to 1.9-fold to that of GaSe. The Ag ions with a larger size compared to Al ions intercalate between growth layers and substitute Ga or interstitial in limited concentrations [4] that results in lower hardness compared to GaSe:Al.

4.2. Optical transmission

The optical transmission curve for GaSe:Al is weakly dependent on Al-doping. Fig. 1a shows that the grown GaSe:Al samples are characterized by the exceeded absorption at wavelength ≤0.62 μm in comparison with the pure GaSe sample. Besides, a small tendency for long-wavelength shift (Fig. 1b) is possibly caused by the defect band(s) and sub-microdispersed inclusions. Insignificant changes in the phonon absorption spectra were found. The optical quality of GaSe:Al crystals is rapidly degrading with increasing Al-doping which is different to that of GaSe:S crystals with S-doping. GaSe:$AgGaS_2$ and GaSe:S (2 mass%) have the same short-wavelength cut of transparency spectrum, but GaSe:$AgGaS_2$ crystal is characterized by negligibly higher optical losses. From the transmission measurements with fs OPA operating at 2.6 μm, it was found that the GaSe:$AgGaS_2$ and GaSe:Al (≤0.05 mass%) samples are characterized by a low absorption coefficient of $\alpha \leq 0.1-0.2$ cm^{-1} at a maximal transparency range, which are very suitable for the mid-IR applications. The thin GaSe:Al (≤0.5 mass%) films with $\alpha \leq 1$ cm^{-1} are still suitable for the nonlinear applications with fs pulse pumping.

4.3. SHG phase matching

The type I SHG of CO_2 laser shows that at $\theta \neq 90°$ the φ-dependent output signal is the six-petal-flower type which is related to $d_{eff} = d_{22} \cos\theta \sin 3\varphi$ for hexagonal ε-GaSe[18]. The thinner samples exfoliated from these crystals also showed the identical φ-dependence, thus, the hexagonal structure in these crystals can be confirmed. The SHG power as a function of the pump beam position on the crystal surface and crystal length l_c shows no domain structure in these crystals.

Fig. 3 shows the diagram of the type I SHG PM versus a pumping wavelength. The experimental SHG PM did not reported yet in GaSe by the pump with wavelength less than 2.36 μm [25]. In this study, we observed the SHG under the pumping by idler waves of fs OPA at 2.12 −2.9 μm. In Fig. 3, the full range of SHG PM for the GaSe crystals are most consistent with the data estimated by using dispersion relations reported in [10,19]. It should be noted that dispersion relations (2) reported in [20], which are valid within 0.75−5 μm range, indicate some overestimated birefringence. As shown in Fig. 4, our experimental data for λ>2.79 μm are in good coincidence with both data estimated from the dispersion relations reported in [10,19] and the majority of published experimental data in [2,19,21,23,24,26] excluding the experimental data reported in [22] for CO_2 laser SHG. Dotted lines outline the common trend in SHG phase matching versus the pump wavelength. The PM angles for 2.5−2.65 μm SHG are shifted to the curve estimated from the dispersion relations in [7] which are valid at 2.4−28 μm range. The PM angles for SHG at 2.25 μm, as the experimental data for SHG at 2.36 μm pump reported in [22], are in good coincidence with the dispersion data in [7,19] but they are 2° larger from the curve estimated by the dispersion relations proposed in [10]. Fig. 4a shows that the SHG PM angles at 2.25−2.9 μm for GaSe:Al are almost identical to that in GaSe. Large SHG PM angles for GaSe and GaSe:Al at 2.12 μm pump have not allowed us to measure PM angles correctly. It is because the high reflectivity of crystal surfaces at PM angles more than 75° decreases the output signals drastically. In this case, the wide spectral bandwidth of the fs pump pulses and the large gradient dθ/dλ lead to some asymmetrical deformation of the SHG pulse spectrum compared to the pump pulse spectrum. It can be concluded that our experimental data for the SHG in GaSe and GaSe:Al are in good agreement with the dispersion relations reported in [10,19] at λ>2.79 μm, while at λ≤2.5 μm pump in agreement only with the data reported in [19]. The PM angles for GaSe:$AgGaS_2$ and GaSe:S (2 mass%) crystals grown by the conventional technique were measured on the whole range of 2.12−2.9 μm and also at CO_2 laser wavelengths. Our experimental data follow the general trend with a

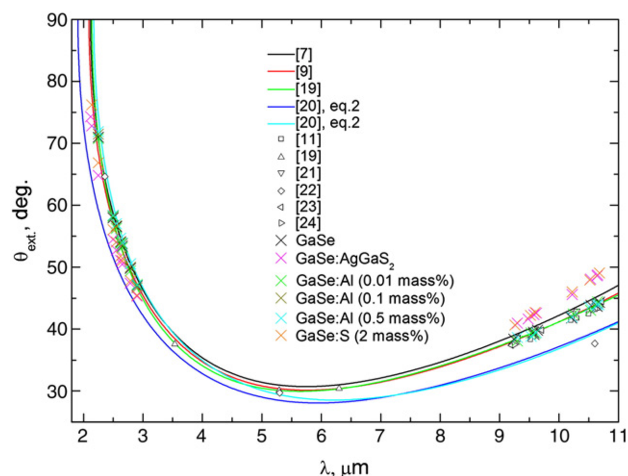

Fig. 3. External PM angle versus pump wavelength for type I SHG in GaSe:$AgGaS_2$, GaSe:Al and GaSe. Lines are theoretical curves, geometric shapes are this study and known as experimental data for type I SHG in GaSe. Inset, crystals observed and references.

Author's personal copy

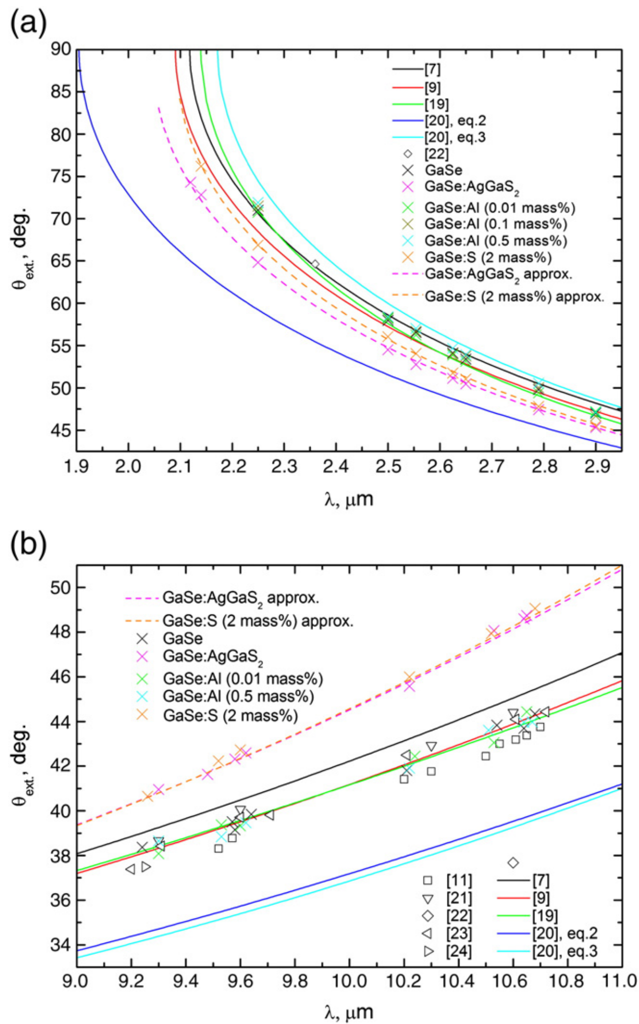

Fig. 4. External PM angle versus pump wavelength for type I SHG in GaSe:$AgGaS_2$, GaSe:Al and GaSe at (a) fs OPA and (b) CO_2 laser pump. Lines are theoretical curves and polynomial approximations, geometric shapes are this study and known as experimental data. Inset, crystals observed and references.

small difference between them that can be due to a small difference in composition.

4.4. Surface damage threshold

Surface damage threshold of the crystals was measured at 2.12−2.9 μm by fs OPA and at 10.6 μm by ns CO_2 laser radiations. The incident and output powers were compared in the measurement. The damage threshold of the pure GaSe sample is estimated at 90 GW/cm^2 and it does not depend on the OPA wavelengths used. The damage threshold of the doped GaSe:Al and all GaSe:S(2 wt.%) crystals measured by fs pulses is about 10−15% lower than that for a pure GaSe crystal. The damage threshold of the GaSe:S sample (10.2 mass%) measured by 150 ns CO_2 laser is 1.4- to 1.5-fold than that of pure GaSe. It is in satisfactory agreement with the damage thresholds reported in [15] for the pure GaSe and GaSe:S (10 mass%) exposed with 14 ns Nd:YAG radiation. However, in difference to [15], we obtained a higher (roughly 1.5- to 1.8-fold) damage threshold of GaSe:S (2 mass%) crystal than that for GaSe:S (10.2 mass%). No difference between damage thresholds of the GaSe:S (2 mass%) samples grown by a conventional doping technique and from the melt GaSe:$AgGaS_2$ were found, so as between pure GaSe and GaSe:Al (≤0.05 mass%).

4.5. Nonlinear coefficient

Nonlinear coefficients were measured by comparing the SHG efficiency of doped GaSe with that of pure GaSe at the pump wavelength of 2.79 μm (fs OPA) with intensity of only 10% of the damage threshold. This pump wavelength and intensity could exclude an influence of nonlinear absorption. As thin as about 0.3 ± 0.02 mm crystals are used to reduce the influence of its optical quality on the measurement results. No significant difference was found experimentally between the nonlinearities of the GaSe:S (2 mass%) grown from the melt GaSe:$AgGaS_2$ and the one by the conventional technology. The results obtained for S-doped GaSe crystals, d_{22}(GaSe:S (2 mass%)) = 0.89·d_{22}(GaSe) and d_{22}(GaSe:S (10.2 mass%)) = 0.8·d_{22}(GaSe), are in good agreement with the results reported in [15]. In the calculation of nonlinear coefficient d_{22}, the θ-angle dependence of d_{eff} was accounted.

Thus, d_{22}(GaSe:S (2 mass%)) is 11% lower than d_{22}(GaSe) leading to about 21% decreasing in the figure of merit and SHG efficiency. On the other hand, this decrease in efficiency will be overcompensated by 50–80% increasing in the damage threshold of GaSe:S (2 mass%) compared to that of pure GaSe. That is why, as high as 1.4-fold efficiency can be predicted for GaSe:S (2 mass%) crystal compared to that in pure GaSe. More over, the SHG PM angle under 2.79 μm pump is about 2° lower in GaSe:S (2 mass%) than that in pure GaSe that leads to further 4.4% increase in d_{eff} and 9% in efficiency. Again, at ns pulse pumping, sub-centimetre or centimetre sized crystals are generally required in order to reach higher SHG efficiency. For example, in such case, up to 35% increase in efficient d_{22} is reported for SHG in 4-mm long GaSe:In compared to that in 4-mm long pure GaSe crystal due to the improved optical quality [3]. The improvement in optical quality was also observed by us in GaSe:S crystals [2]. All together, the above mentioned factors can explain the 2.4-fold higher of Er^{3+}:YSGG laser SHG efficiency in GaSe:S (2 mass%) as reported in [2] to that in pure GaSe. We can conclude that the advantages of the crystal grown from the melt GaSe:$AgGaSe_2$ with regards to SHG efficiency compared to that in pure GaSe crystals reported in [4] can own the same origin.

The SHG efficiency as a function of dopant, doping level, pump intensity, and crystal length with fs OPA pump indicates a too complicated dependence that is why no attempt was made to maximize it. Nevertheless, for the majority of 0.5−1 mm crystals, including crystals grown from the melt GaSe:$AgGaS_2$ the SHG average output power of ≥ 15 ± 3 mW is measured under the pumping with 105 mW fs OPA output at 2.4 μm central wavelength. The pump intensity is well below the damage threshold.

5. Conclusion

We have reported the physical properties of the crystals grown from the melt GaSe:$AgGaS_2$ (10.6 wt.%) and GaSe:Al (0.01, 0.05, 0.1, 0.5, 1, 2 wt.%) in charge composition. The crystal grown from the melt GaSe:$AgGaS_2$ (10.6 wt.%) is identified as the GaSe:S (2 mass%) crystal with more uniform S-distribution and almost the same optical quality compared to that in GaSe:S (2 mass%) grown by the conventional technique. Both GaSe:S (2 wt.%) crystals are characterized by the almost identical transparency curve and SHG PM diagram that are shifted to short-wavelength range in comparison with pure GaSe. 11% lower second order nonlinear susceptibility coefficient d_{22} of these doped crystals was measured as compared to that in pure GaSe. Nevertheless, both of them possess higher efficiency in SHG than that in pure GaSe due to a higher optical quality and damage threshold, modified phase matching conditions and other physical properties. GaSe:S crystals possess the best set of physical properties for the frequency conversion within mid-IR among doped GaSe crystals at 2−3 wt.% S-doping. In addition, GaSe:S (2 wt.%) crystals grown from the melt GaSe:$AgGaS_2$ can be cut and polished at arbitrary direction because of its good hardness property, which can find many important applications for out-door

Author's personal copy

experiments. GaSe:Al (≤0.05 wt.%) crystals possess optical quality close to pure GaSe up to 2.5−3-folded hardness than that of pure GaSe and 25% higher than GaSe:S (2 wt.%) grown from the melt GaSe:$AgGaS_2$ and extremely low conductivity of $\leq 10^{-7}$ Om^{-1} cm^{-1}. Low conductivity makes GaSe:Al significantly attractive for THz applications.

Acknowledgment

This work is partially supported by NSFC (No.10774059) and the National Basic Research Program (2006BC921103) of China, Presidium SB RAS under the Project VII.63.3.1 of VII.63.3 Program, FPP under Country Contract No.02.740.11.0444, Presidential Grant SS-4297.2010.2 and RFBR Project No. 10-02-01452-a.

References

[1] K.R. Allakhverdiev, R.I. Guliev, E.Yu. Salaev, V.V. Smirnov, Sov. J. Quantum Electron. 12 (1982) 947.
[2] H.Z. Zhang, Z.H. Kang, Yu. Jiang, J.Yu. Gao, F.G. Wu, Z.S. Feng, Yu.M. Andreev, G.V. Lanskii, A.N. Morozov, E.I. Sachkova, S.Yu. Sarkisov, Opt. Exp. 16 (2008) 9951.
[3] D.R. Suhre, N.B. Singh, V. Balakrishna, N.C. Fernelius, F.K. Hopkins, Opt. Lett. 22 (1997) 75.
[4] N.B. Singh, D.R. Suhre, W. Rosch, R. Meyer, M. Marable, N.C. Fernelius, F.K. Hopkins, D.E. Zelmon, R. Narayanan, J. Cryst. Growth 198 (1999) 588.
[5] Z.S. Feng, Z.H. Kang, F.G. Wu, J.Yu. Gao, Yu. Jiang, H.Z. Zhang, Yu.M. Andreev, G.V. Lanskii, V.V. Atuchin, T.A. Gavrilova, Opt. Exp. 16 (2008) 9978.
[6] Yu.K. Hsu, Ch.W. Chen, Ju.Y. Huang, C.L. Pan, J.Yu. Zhang, Ch.Sh. Chang, Opt. Exp. 14 (2006) 5484.
[7] Ch.W. Chen, Yu.K. Hsu, J.Y. Huang, Ch.Sh. Chang, J.Yu. Zhang, C.L. Pan, Opt. Exp. 14 (2006) 10636.
[8] Ch.W. Chen, T.T. Tang, S.H. Lin, J.Y. Huang, Ch.Sh. Chang, P.K. Chung, Sh.T. Yen, C.L. Pan, J. Opt. Soc. Am. B 26 (2009) A58.
[9] A.A. Tikhomirov, Yu.M. Andreev, G.V. Lanskii, O.V. Voevodina, S.Yu. Sarkisov, SPIE Proc. 6258 (2006) 64.
[10] K.L. Vodopyanov, L.A. Kulevskii, Opt. Commun. 118 (1995) 375.
[11] S. Das, Ch. Ghosh, O.G. Voevodina, Yu.M. Andreev, S.Yu. Sarkisov, Appl. Phys. B 82 (2006) 43.
[12] S. Das, Ch. Ghosh, S. Gangopadhyay, U. Chatterjee, G.C. Bhar, V.G. Voevodin, O.G. Voevodina, J. Opt. Soc. Am. B 23 (2006) 282.
[13] Yu.M. Andreev, V.V. Atuchin, G.V. Lanskii, A.N. Morozov, L.D. Pokrovsky, S.Yu. Sarkisov, O.V. Voevodina, Mat. Sci. Eng. B 128 (2006) 205.
[14] S.A. Ku, C.W. Luo, H.L. Lio, K.H. Wu, J.Y. Juang, A.I. Potekaev, O.P. Tolbanov, S.Yu. Sarkisov, Yu.M. Andreev, G.V. Lanskii, Russ. Phys. J. 51 (2008) 1083.
[15] V. Petrov, V.L. Panyutin, A. Tyazhev, G. Marchev, A.I. Zagumennyi, F. Rotermund, F. Noack, Proceedings of the 17th Int. Conf. on Advanced Laser Technologies, Antalya, Turkey, 2009, p. 210.
[16] V.L. Panyutin, A.I. Zagumennyi, A.F. Zerrouk, F. Noack, V. Petrov, Proceedings of the Conf. on Lasers and Electro-Optics/Int. Quantum Electron., Baltimore, Maryland, 2009.
[17] A. Gouskov, J. Camassel, L. Gouskov, Prog. Cryst. Growth Charact. Mater. 5 (1982) 323.
[18] Yu.M. Andreev, K.A. Kokh, G.V. Lanskii, A.N. Morozov, Structural characterization of pure and doped GaSe by nonlinear optical method, J. Cryst. Growth. (in press), doi:10.1016/j.jcrysgro.2010.10.194.
[19] E. Takaoka, K. Kato, Jap. J. Appl. Phys. 38 (1999) 2755.
[20] K.R. Allakhverdiev, T. Baykara, A. Kulibekov Gulubayov, A.A. Kaya, J. Goldstein, N. Fernelius, S. Hanna, Z. Salaeva, J. Appl. Phys. 98 (2005) 093515.
[21] G.B. Abdullaev, K.R. Allakhverdiev, M.E. Karasev, V.I. Konov, L.A. Kulevskii, N.B. Mustafaev, P.P. Pashinin, A.M. Prokhorov, Yu.M. Starodumov, N.I. Chapliev, Sov. J. Quantum Electron. 19 (1989) 494.
[22] G.B. Abdullaev, L.A. Kulevskii, A.M. Prokhorov, A.D. Savel'ev, E.Yu. Salaev, V.V. Smirnov, JETP Lett. 16 (1972) 90.
[23] G.C. Bhar, S. Das, K.L. Vodopyanov, Appl. Phys. B 61 (1995) 187.
[24] N.B. Singh, D.R. Suhre, V. Balakrishna, M. Marable, R. Meyer, N. Fernelius, F.K. Hopkins, D. Zelmon, Prog. Cryst. Growth Charact. Mater. 37 (1998) 47.
[25] N.C. Fernelius, Prog. Cryst. Growth Charact. Mater. 28 (1994) 275.
[26] J.M. Auerhammer, E.R. Eliel, Opt. Lett. 21 (1996) 773.